

PAPER

Design and performance analysis of eight channel demultiplexer using 2D photonic crystal with trapezium cavity






To cite this article: V Kavitha *et al* 2023 *J. Opt.* **25** 065102

View the [article online](#) for updates and enhancements.

You may also like

- [Induced transparency based subwavelength acoustic demultiplexers](#)
Tianyu Gu, Yi Cheng, Zhihui Wen et al.
- [Heterostructure based demultiplexer using solid–solid phononic crystal ring resonators](#)
Javad Babaki and Fakhroddin Nazari
- [Design of a 1 × 4 silicon-alumina wavelength demultiplexer based on multimode interference in slot waveguide structures](#)
Dror Malka, Yoav Sintov and Zeev Zalevsky

Design and performance analysis of eight channel demultiplexer using 2D photonic crystal with trapezium cavity

V Kavitha^{1,*} , V R Balaji² , Shanmuga Sundar Dhanabalan³ , T Sridarshini⁴, S Robinson¹, Massoudi Radhouene⁵, Gopalkrishna Hegde⁶ , and R G Jesuwanth Sugesh⁷ 

¹ Mount Zion College of Engineering and Technology, Pudukkottai, Tamil Nadu, India

² School of Electronics Engineering, School of Electronics Engineering, Vellore Institute of Technology, Chennai, Tamil Nadu, India

³ Functional Materials and Microsystems Research Group, School of Engineering, RMIT University, Melbourne, Victoria, Australia

⁴ Department of Electronics and Communication Engineering, PSG College of Technology, Coimbatore, Tamil Nadu, India

⁵ University of Tunis El Manar, National Engineering School of Tunis Communication Systems LR-99-ES21, Tunis, Tunisia

⁶ Center for Bio Systems Science and Engineering, Indian Institute of Science, Bengaluru, Karnataka, India

⁷ Department of Electronics and Communication Engineering, School of Engineering and Technology, CHRIST University, Bengaluru, Karnataka, India

E-mail: kavithamzion@gmail.com

Received 16 October 2022, revised 17 April 2023

Accepted for publication 20 April 2023

Published 10 May 2023



CrossMark

Abstract

In this work, an eight-channel dense wavelength division multiplexing demultiplexer is designed with a 2D photonic crystal triangular lattice. The proposed demultiplexer consists of a centre bus waveguide, an isosceles trapezium resonant cavity, and an eight-circular ring cavity (CR1, CR2, CR3, CR4, CR5, CR6, CR7, and CR8). The point defect resonant cavity consists of seven rods to drop different wavelengths from eight cavities, each of eight drop waveguides. The design is very simple to realise. The finite difference time domain and plane wave expansion method methods were used to analyse the proposed design's band structure and transmission spectrum. The resonant wavelengths are 1.5441 μm , 1.5443 μm , 1.544 49 μm , 1.5447 μm , 1.5449 μm , 1.5451 μm , 1.5453 μm , and 1.5455 μm respectively. The proposed device provides a high-quality factor, transmission efficiency, and low crosstalk. The device's footprint is 490.0 μm^2 , which can be easily incorporated into photonic integrated circuits.

Keywords: DWDM demultiplexer, photonic crystal, resonant wavelength, quality factor, trapezium, crosstalk

(Some figures may appear in colour only in the online journal)

* Author to whom any correspondence should be addressed.

1. Introduction

Due to the rapid growth in the number of data users and need for increased bandwidth optical communications is preferred over radio frequencies to realize ultra-high-speed networks [1]. The key technologies supporting the current communication systems are electronics and photonics. Electrons play a significant role in electronics, and photons play a crucial role in photonics. Many advanced fabrication technologies were in industry today, leading to a drastic reduction in the device's size. Initially, in electronic vacuum tubes, transistors were more prominent in size to enhance performance and size reduction [2]. The integrated circuits were developed with the dimensions of small-scale, medium-scale, and large-scale integration technology and come to market for device minimization [3]. Device minimization plays a significant role in nanotechnology. The current device sizes are 10 nm and 7 nm, and are expected to be reduced to 5 nm and 2 nm. Recent progress in nanotechnology has reduced the device's size to the nanoscale and the amount of power required, thus improving device performance [4].

In photonics, initial development started with discrete fibre optic components [5], and many devices are available today in optics to support the optical circuits. The device's size is significant for developing optical devices with small size, ultra-fast, high speed, low power dissipation, ultra-high bandwidth communication, and long life in the photonic integrated circuit (PIC) [6]. The key technologies developed for device miniaturization in the PIC are planar lightwave circuits (PLCs) and micro electro mechanical systems (MEMS). The PLC device can be fabricated on a single chip but with footprint in millimetres. Other technology in MEMS reduces the device to micrometres [7]. The major drawback to MEMS is lifespan and light scattering and achievable size of the structure.

Photonic crystal (PC) is an alternative technology for supporting photonic integrated circuits. The microstructure of photonic materials that can modulate the propagation states of photons is one essential requirement of integrated photonic technology. The unique properties of a PC are the photonic bandgap. The photonic bandgap originates from the modulation of light by a spatially periodic distribution of dielectric constant [8]. Further, the density of propagation of photons is zero in the photonics band gap (PBG) band, and it acts as a reflector while not introducing defects [9]. The PBG, which appears in the optical communication band ranging from 1260 nm to 1625 nm, is the main inspiration for the industry to build the fundamentals of integrated circuits using PCs. The PC can allow light into PBG by introducing a defect in the crystal that is by breaking the periodicity. The propagation of light in PBG enables the design of various components like fibre optics [10], filters [11], lasers [12], multiplexers [13], demultiplexers [14], routers [15], logic gates [16], power splitters [17], and optical sensors [18].

Wavelength division multiplexing (WDM) is an essential technology in optical communication systems. The WDM allows the single-mode fibre (SMF) to carry several wavelengths per fibre. WDM is divided into coarse WDM (CWDM) and dense WDM (DWDM). CWDM

(ITU-T G.694.2) uses a larger channel spacing (20 nm) and is insufficient to support more users than DWDM (ITU-T G.694.1). The channel spacing in DWDM ranges from 0.1 nm (12.5 GHz) to 1.6 nm (200 GHz), with a maximum of 1200 channels at 12.5 GHz (0.1 nm) and a minimum of 75 channels at 1.6 nm (200 GHz) [19].

In an optical communication system, the demultiplexer is the prominent device at the receiver end to select the specific channel at the unique wavelength. The conventional demultiplexer [20] occupies more space, more power and high scattering losses. The industry is looking for a PC-based demultiplexer to support more channels in a small footprint, low power requirements, higher transmission efficiency, and low crosstalk [21]. Rostami *et al* [22] designed a four-channel demultiplexer using a Y-shaped waveguide and resonant cavity. The model exhibits wavelength shift by varying the defect radius inside the cavity. The design had a maximum efficiency of 92%, a quality factor of 1724, and minimum crosstalk of -33.18 dB, respectively. The drawbacks are large channel spacing around 3.2 nm and efficiency is not flat, it has a minimum and maximum efficiency of 60% and 92%, respectively. The dual-channel demultiplexer is designed and reported by Alipour-Banaei *et al* [23]. The structure consists of a point defect resonant cavity and input and output waveguide. The desired wavelength is dropped by adjusting the radius of the reduced rod inside the cavity. The demultiplexer is designed to drop the wavelength with a maximum transmission efficiency of 92% and a quality factor of 3000. Mohammadi *et al* [24] designed the four-channel demultiplexer. The design consists of four X-shaped cavities and scattering rods. The desired wavelength is dropped by varying the radius of the scattering rods. The design had a maximum transmission efficiency of 63%, a maximum quality factor of 1954, and minimum Crosstalk of 22.7. Cons of this design is the high power loss and minimum transmission efficiency of 45%. Rastegarnia [25] designed the two-channel demultiplexer. This design provides a high-quality factor of 7854, transmission efficiency of 100% and crosstalk of -26 dB, respectively. Mehdizadeh and Soroosh [26] devised a four-channel demultiplexer using a hexagonal resonator. The demultiplexer is designed to drop the desired wavelength by adjusting the inner rod of the resonator through the drop waveguide. The design provides the maximum transmission efficiency, spectral width, and crosstalk are all 100%, 0.7 nm, and -27 dB. Fallahi *et al* [27] designed the four-channel demultiplexer. The design consists of a resonant cavity and an input and output waveguide. The desired wavelength is dropped by varying the defect rod radius in the centre of the cavity. This design provides a channel spacing of 13 nm and a minimum spectral width of 2.5 nm. The minimum transmission efficiency is 73%, and the low crosstalk is -43.9 dB.

Fallahi and Seifouri [28] devised a four-channel demultiplexer. The desired wavelength is dropped by varying the inner rods of the ring resonator. This design provides a channel spacing of 2.7 nm and a minimum spectral width of 2.5 nm. The minimum transmission efficiency is 92%, and the low crosstalk is -36.5 dB. The same author [29] proposed an eight-channel demultiplexer using a triangular lattice. The

design provides high transmission efficiency for all channels, but the performance parameter quality factor is deficient. Channel spacing is variable between the channels. From the literature survey [22–31], we observe that the existing work in the PC demultiplexer employs line defect waveguides, point defects, and resonant cavities in the shapes of a circular, hexagonal, x-shaped, quasi-circular, flower shape, square shape, or octagonal. Many of the proposed and designed papers in PC DWDM demultiplexer lacks some of the requirements of ITU-T G.694.1. The requirements are a high-quality factor, narrow spectral width, uniform transmission efficiency, uniform channel spacing, less Crosstalk, and ultra-compact size.

In this work, we have attempted to incorporate the standards of ITU-T G.694.1 into the proposed DWDM demultiplexer by improving the performance parameters of the demultiplexer and explored to improve the shortfall in the already existing demultiplexer. The eight-channel demultiplexer is designed using an isosceles trapezium cavity, and the design is realistic and simple in a triangular lattice for fabrication. To the best of our knowledge, this is the first time a proposed trapezium cavity demultiplexer has been designed. The resonator and cavity are simple. After several iterations and completing the study of band gap analysis, the design can show promising results in terms of high-quality factor ≥ 8000 , narrow spectral width $\leq 0.0002 \mu\text{m}$, uniform transmission efficiency $\geq 90\%$, uniform channel spacing, less Crosstalk $\geq -50 \text{ dB}$, and ultra-compact size.

The paper is structured as follows. In section 2, we described the bandgap analysis of the demultiplexer. The design of the 2D PC demultiplexer and structural parameters are given in section 3. Section 4 presents the analysis, discussion on the structural parameters and results. Section 5 concludes our research.

2. Bandgap analysis

Figure 1 shows an array of rods in a triangular lattice for modelling an eight-channel demultiplexer. There are 40 rods in the X direction and a 37-rod array in the Z direction. The proposed structure is simulated using the plane wave expansion method to obtain the PBG.

In this design, the 2D PC comprises a triangular lattice of gallium arsenide (GaAs) dielectric circular rods on an air background. The demultiplexer is designed with 41 rods in the X direction and 37 rods in the Z direction. The rod with a refractive index of $n_{\text{GaAs}} = 3.4$, which corresponds to GaAs at the canonical wavelength of $1.55 \mu\text{m}$ [8] is immersed in the air (background index $n_{\text{air}} = 1$). The index difference is calculated to be $2.4 (\Delta n = n_{\text{GaAs}} - n_{\text{air}})$. The non-defect rod radius (R) is 105 nm , and the lattice constant (a) is $0.6 \mu\text{m}$. The PBG is calculated and displayed in figure 2 before introducing the defects.

According to figure 2(a), the dotted red lines show the allowed transverse magnetic (TM) modes (and the blue lines show the transverse electric (TE) modes), but these modes are not falling in the region of optical communication frequency. The hexagonal lattice provides a broader PBG than the

square lattice and better light confinement and is used for the proposed structure. Figure 2(a) shows the two TE PBG and one TM PBG. The first TE PBG band extends from $0.27605 < a/\lambda < 0.44715$, and the corresponding wavelength range between $1274.74 \text{ nm} < \lambda < 2064.84 \text{ nm}$, the second TE PBG appears at $0.5635 < a/\lambda < 0.59316$ and ranges of wavelength between $960 \text{ nm} < \lambda < 1011.53 \text{ nm}$. The TM PBG band extends from $0.82129 < \lambda < 0.86692$, equal to $657.5 \text{ nm} < \lambda < 694.03 \text{ nm}$. The first TE PBG covers the range of conventional C-window optical communication and is used for the proposed demultiplexer. The band diagram after introducing defects in the 40×73 lattice is shown in figure 2(b). The defects break the PBG, allowing the guided mode to propagate in the normalized frequency range of $0.27605 < a/\lambda < 0.44715$.

3. Proposed DWDM demultiplexer and working principle

Figure 3 shows the schematic of proposed demultiplexer, designed with an array of 41×37 dielectric rods. The proposed design is simple in terms of fabrication feasibility. The minimum rod radius used in the proposed design is $0.1 \mu\text{m}$. The demultiplexer is designed using a triangular lattice. The trapezoid cavity is obtained by introducing linear defects in the triangular lattice. To the best of our knowledge, the report paper did not use the structure of a trapezoid cavity in the demultiplexer.

The demultiplexer consists of four inverted trapezium-shaped cavities, eight circular ring cavities (CRs), eight drop waveguides, single bus waveguides, and a reflector rod. Two trapezoid cavities are used on the top, and another two cavities are placed on the bottom. In the left and right corners of the cavity, a CR is designed. The wide beam of signal propagates through the bus waveguide, and the demultiplexer is designed to drop eight ITU standard wavelengths by changing the rod radius of the CR cavity. The eight-drop waveguide drops the eight different wavelengths, each placed above and below the CR cavity.

The bus waveguide is created in the crystal by removing the 34 rods in their respective positions, as shown in figure 3. The wide beam of Gaussian signal with a centre wavelength of 1550 nm propagates through the bus waveguide at different frequencies. The reflector row of rods (7 rods) is placed at the right end of the bus waveguide. The reflector introduced in the proposed design helps to enhance more EM waves coupled to the resonator and also helps to increase the transmission efficiency of the resonant wavelength.

The resonator in the proposed demultiplexer based on the isosceles trapezium resonant cavity (ITRC) is designed by deleting $(10 + 4 + 4 + 5)$ rods in the respective position, shown in figure 3. The resonator couples the light to each cavity from the bus waveguide and allows it to circulate inside the cavity. The mean trip time of the trapezoid cavity is equal to integral multiples of 2π (1), builds the strong electric field around the cavity through constructive interference and allows the multiple frequencies to resonate inside the cavity,

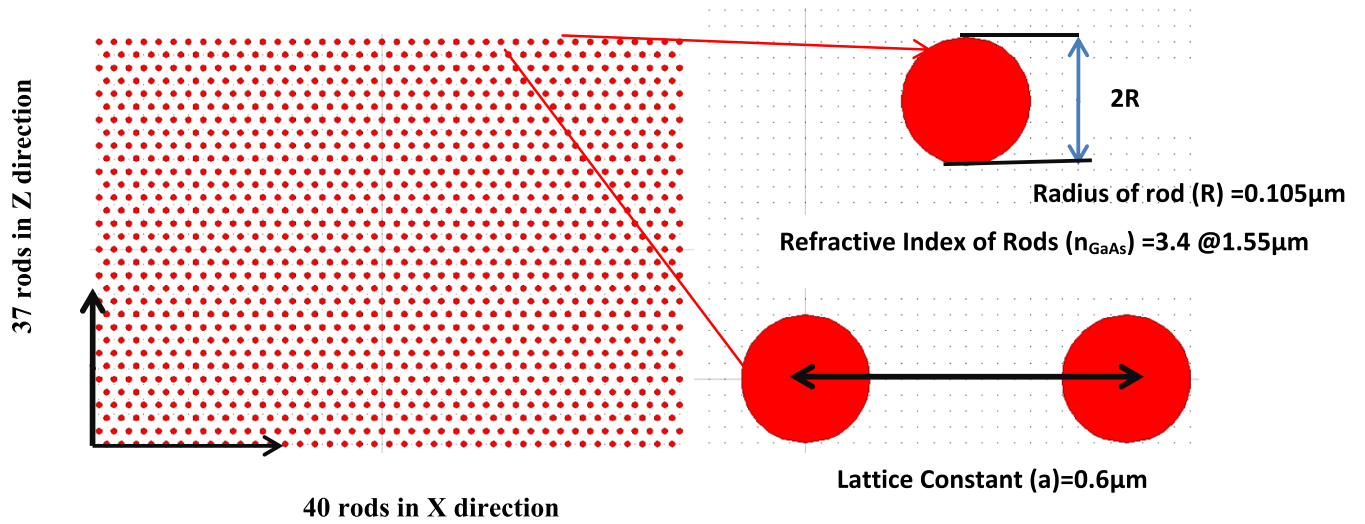


Figure 1. 40×37 2D PC structure for proposed demultiplexer.

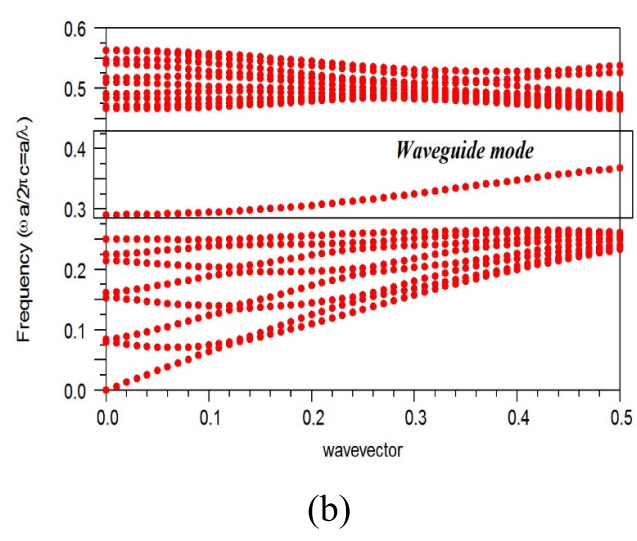
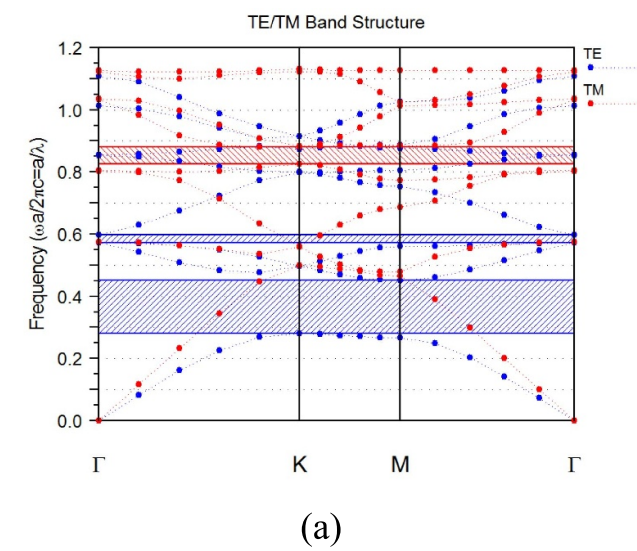


Figure 2. Band diagram of 37×41 rods (GaAs) (a) before defects and (b) after the defect.

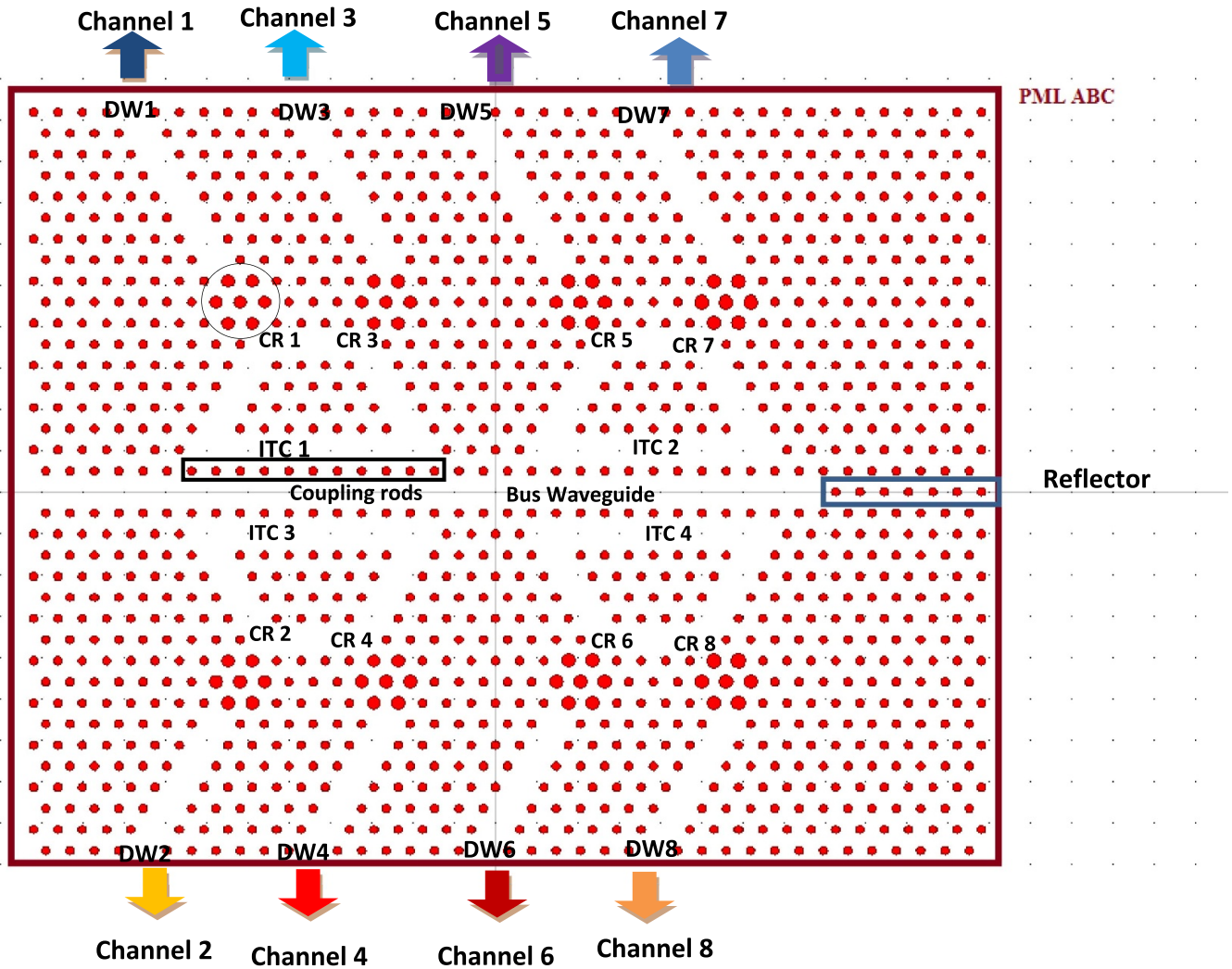


Figure 3. Schematic of the proposed eight-channel DWDM demultiplexer design. CR: circular resonant; ITC: isosceles trapezium cavity; DW: drop waveguide.

$$2\pi r = n\lambda \tag{1}$$

where, n is the mode number, λ is the guided wavelength, and r is the radius of the resonator.

The CR cavity acts as a filter in the proposed design. Nine rods are used to design the cavity, as shown in figure 3. The CR cavity, which is the primary element in the demultiplexer, is designed using point defects. The CR cavity limits the resonant wavelength from the resonator only at a specific frequency. The cavity is optimized to drop the high Q value resonant wavelength based on the rod radius of the nine rods. The drop waveguide is created in the crystal by introducing the line defect by removing the eight rods in the respective positions, as shown in figure 3. The drop waveguide is used to drop the resonant wavelength. From the bus waveguide, one of the frequencies drops to the drop waveguide through the resonator and CR cavity. The detailed structural parameter of the proposed design is shown in table 1.

According to figure 3, light from SMF enters into the demultiplexer through the bus waveguide, which permits transmitting different resonant frequencies. The resonators

(trapezium) couple the incoming light through coupling rods, building the high-intensity field due to the constructive interference and circumference of the trapezium cavity (ITR). Each resonator has two CR cavities located on the right and left ends of the resonator. Based on the radius of the CR cavity, a specific wavelength matches, and the corresponding frequency is resonant and trapped with the cavity mode trapped by the cavity and transferred to the drop waveguide by the concept called photon tunnelling resonant effect.

4. Simulation results, analysis and discussion

Finite difference time domain (FDTD) is one of the simplest and most powerful algorithms for modelling PC structures and works with Maxwell's equations [32]. The meshed 3D FDTD requires more time for simulation and powerful computers. To reduce the complexity, the proposed design is simulated with 2D FDTD using the effective index method to reduce errors to a minimum. For precise calculations, FDTD requires precise

Table 1. Structural parameters of the proposed eight-channel demultiplexer.

Structural parameters	Quantity/unit	Symbol
TE ₁ gap (frequency)	$0.276\ 05 \times 2\pi c/a$ to $0.447\ 15 \times 2\pi c/a$	ω
TE ₁ gap (wavelength)	$1.274\ 74\ \mu\text{m} < \lambda < 2.064\ 84\ \mu\text{m}$	λ
TE ₂ gap (frequency)	$0.5635 \times 2\pi c/a$ to $0.593\ 16 \times 2\pi c/a$	ω
TE ₂ gap (wavelength)	$0.960\ \mu\text{m} < \lambda < 1.011\ 53\ \mu\text{m}$	λ
TM ₁ gap (frequency)	$0.821\ 29 \times 2\pi c/a$ to $0.866\ 92 \times 2\pi c/a$	ω
TM ₁ gap (wavelength)	$0.6575\ \mu\text{m} < \lambda < 0.694\ 03\ \mu\text{m}$	λ
Band (conventional window)	$1.530\text{--}1.565\ \mu\text{m}$ (Covers in TE ₁ gap)	nm
Mid band wavelength (Gaussian source)	$1.550\ \mu\text{m}$	λ_r
Non-defect rod radius	$0.105\ \mu\text{m}$	r
Diameter of rod radius	$0.210\ \mu\text{m}$	d
Lattice constant	$0.6\ \mu\text{m}$	a
Background index in air	1	n_a
The refractive index of GaAs dielectric rods at 1550 nm	3.4	n_{GaAs}
Refractive index difference	2.46	$\Delta n = n_{\text{GaAs}} - n_{\text{air}}$
Mesh size	$\Delta x = \Delta z = a/20$	—
PML ABC	$0.5\ \mu\text{m}$	—
FDTD grid	$0.02\ \mu\text{m}$	Δ
Time step (stability factor)	0.022 403	(Δt)
No. of rods in X direction	41	N_x
No. of rods in Z direction	37	N_z
Height of rod	2000	H
Total no. of rods in device	1517	—
Size	$490.0\ \mu\text{m}^2$	—
Total no. of channels	8	—
Isosceles trapezium resonant cavity (ITRC)	$0.105\ \mu\text{m}$	NA
No of ITRC in the proposed design	4	—
No of circular ring cavity (CR)	8	NA
Channel 1 (25 GHz) (0.0002 μm)	$0.140\ \mu\text{m}$	CR1
Channel 2 (25 GHz) (0.0002 μm)	$0.145\ \mu\text{m}$	CR2
Channel 3 (25 GHz) (0.0002 μm)	$0.150\ \mu\text{m}$	CR3
Channel 4 (25 GHz) (0.0002 μm)	$0.154\ \mu\text{m}$	CR4
Channel 5 (25 GHz) (0.0002 μm)	$0.159\ \mu\text{m}$	CR5
Channel 6 (25 GHz) (0.0002 μm)	$0.165\ \mu\text{m}$	CR6
Channel 7 (25 GHz) (0.0002 μm)	$0.170\ \mu\text{m}$	CR7
Channel 8 (25 GHz) (0.0002 μm)	$0.174\ \mu\text{m}$	CR8

mesh size, perfect matched layer absorbing boundary condition width, and reflectance and time calculations required to match simulation output with the real-time systems.

The FDTD simulation uses the PML ABC algorithm and an artificial absorbing layer designed to absorb the entire incident wavelength with minimal reflections inside the proposed PC structure. The proposed system uses the precise mesh size of $\Delta x = \Delta z = a/20 = 0.03\ \mu\text{m}$ (lattice constant of $0.6\ \mu\text{m}$). The time step is measured using the following equation (2) [33],

$$\Delta t \leq \frac{1}{c\sqrt{\frac{1}{\Delta x^2} + \frac{1}{\Delta y^2}}}. \quad (2)$$

The design uses a time step of 0.0224 fs to provide a stable output. Inaccurate time leads to measuring the fluctuation output by the power monitor, which is very important while modelling the DWDM devices. In order to drop narrow spectral width in the PC demultiplexer, it is vital to increase the number of rods between the bus and the drop waveguide and to reduce

the vertical power losses inside the lattice. The Gaussian input source is launched in the input port with the incremental frequency limit of $0.0001\ \mu\text{m}$ from $1.530\ \mu\text{m}$ to $1.560\ \mu\text{m}$. The memory size of the proposed design is 40 MB, with a simulation time of 2500 min.

The proposed design uses precise mesh size, and the input Gaussian modulated continuous wave l with TE polarisation is launched from the input port shown in figure 3. The power monitor is placed in the eight-drop waveguide. Each port's output spectrum (transmission vs wavelength) is calculated using the FDTD. The output transmission spectrum is calculated using the following equation (3) [33],

$$T(f) = \frac{1/2 \int \text{real}(p(f)^{\text{monitor}}) dS}{\text{SourcePower}} \quad (3)$$

where $T(f)$ denotes normalized transmission as a function of wavelength, $p(f)$ is the Poynting vector, and dS denotes the surface normal to keep the time step precisely.

Transmission efficiency is determined by the ratio of output power to input power. The following equation (4) measures transmission efficiency,

$$TE(\%) = \frac{P_{out}}{P_{in}} \times 100. \quad (4)$$

The P_{out} represents the output power in the receiver port, and the P_{in} represents the transmitted power from the input source.

The 2D FDTD computation algorithm is performed for the proposed device to determine the intensity of transmission spectral power in each drop waveguide of the eight ports, which the time monitor measures. The performance parameters of a demultiplexer are generally determined based on the structural parameters of the design. The performance parameters of the demultiplexer are transmission efficiency, spectral width, quality factor (Q), and crosstalk. The design consists of four resonators and eight circular resonant cavities. In the top, the first trapezium resonator, along with CR1 and CR3, drops the resonant wavelengths at $\lambda_1 = 1.5441 \mu\text{m}$ and $\lambda_3 = 1.5449 \mu\text{m}$ with a transmission efficiency of 97% and 100% and a spectral width of 0.2 nm. The rod radii of CR1 and CR3 are $0.14 \mu\text{m}$ and $0.15 \mu\text{m}$, respectively.

The second resonator, along with CR5 and CR7, drops the resonant wavelength to $1.5449 \mu\text{m}$ and $1.5453 \mu\text{m}$, respectively, with transmission efficiencies of 100% and 100% and spectral width of 0.2 nm. The rod radii of CR5 and CR7 are $1.59 \mu\text{m}$ and $1.70 \mu\text{m}$, respectively. One of the salient features of the proposed design is that the top two ITRCs are designed to drop the odd channels (Channel 1, 3, 5, 7). The two resonators are placed on the bottom side to drop the even channels. The first resonator at the bottom, along with CR2 and CR4, drops the resonant wavelengths at $1.5443 \mu\text{m}$ and $1.5447 \mu\text{m}$ with a transmission efficiency of 99% and 100% and a spectral width of 0.2 nm. The rod radii of CR2 and CR4 are $1.45 \mu\text{m}$ and $1.54 \mu\text{m}$, respectively.

The second resonator, along with CR6 and CR8, drops the resonant wavelength to $1.5451 \mu\text{m}$ and $1.5455 \mu\text{m}$, respectively, with transmission efficiencies of 90% and 100% and spectral width of 0.2 nm. The rod radii of CR6 and CR8 are $1.65 \mu\text{m}$ and $1.74 \mu\text{m}$, respectively. The bottom two ITRCs are designed to drop the even channels (Channel 2, 4, 6, 8). The normalized transmission spectrum of an eight-channel DWDM demultiplexer's transmission efficiency is shown in figure 4. The eight resonant peaks are obtained from the eight CR cavity through the demultiplexer at resonant wavelengths of $1.5441 \mu\text{m}$, $1.5443 \mu\text{m}$, $1.5449 \mu\text{m}$, $1.5447 \mu\text{m}$, $1.5449 \mu\text{m}$, $1.5451 \mu\text{m}$, $1.5453 \mu\text{m}$, and $1.5455 \mu\text{m}$. The details about the structure parameters of the CR cavity and performance parameters are given in table 2.

The channel spacing difference between peaks of the resonant wavelength and the spectral width is the difference between full width and half maximum (FWHM). The quality factor of the transmission spectrum is measured by the resonant wavelength based on the FWHM. The quality factor is calculated using

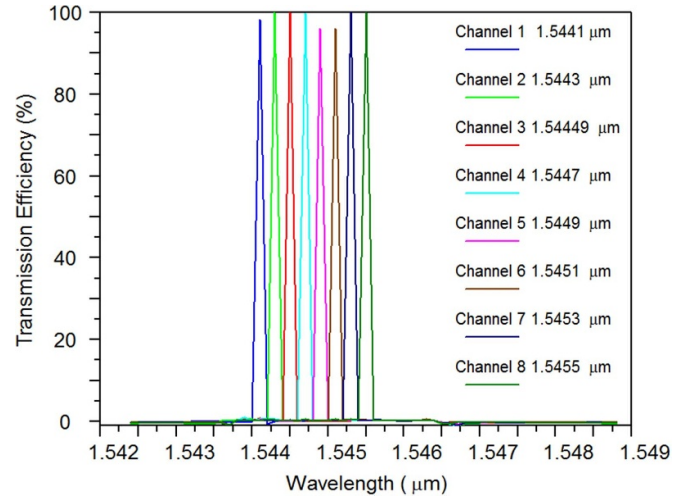


Figure 4. Output spectra for eight-channel DWDM demultiplexer transmission efficiency.

$$Q = \frac{\lambda_r}{\Delta\lambda} = \frac{\text{Resonant Wavelength}}{\text{FWHM}}. \quad (5)$$

Crosstalk is an important parameter for studying the performance analysis of the demultiplexer. Crosstalk is the interference from other channel wavelengths with the present channel, measured in decibels (dB). The crosstalk of the proposed demultiplexer is given in table 3. The proposed design reduces the crosstalk to low values by considering (i) designing the demultiplexer to drop the odd and even channels separately. (ii) Devising the trapezoid cavities on the top to drop the odd channels (Channel 1, Channel 3, Channel 5, and Channel 7) and the bottom to drop the even channels (Channel 2, Channel 4, Channel 6, and Channel 8). The novel idea of reducing the crosstalk between the adjacent channels is achieved in the proposed design. Further, in the left and right corners of the cavity, CR is designed. The CR cavity consists of seven rods whose radii are optimized with several iterations to give less than $0.0002 \mu\text{m}$.

The proposed design provides minimum crosstalk of -64 dB and maximum crosstalk of -44 dB , which is much less than the existing demultiplexer [8, 22–31]. According to figure 5, the transmission spectrum in dB for an eight-channel demultiplexer is shown to determine the crosstalk between the channels. The crosstalk is measured between the desired and adjacent resonant wavelengths. The negative value determines the value of crosstalk. The larger the negative value, the less crosstalk; the higher the negative value, the higher the crosstalk. The following equation (6) measures the crosstalk,

$$\text{Crosstalk (dB)} = 10 \log \left[\frac{P_{out}}{P_{in}} \right]. \quad (6)$$

The P_{out} represents the output power in the receiver port, and the P_{in} represents the transmitted power from the input source [34].

The electric field distribution of odd and even channels is shown in figure 6. Several signal lights at different resonant

Table 2. Structural parameters of CR rod radius and simulation results of eight channel demultiplexer.

Channel spacing (μm)	CR cavity rod radius (μm)	Channel	Resonant wavelength (μm)	Spectral width ($\Delta\lambda$) in (μm)	Q factor	Transmission efficiency (%)
0.0002	CR1	Odd	1.5441	0.0002	7721	97
0.0019	CR3		1.544 49	0.0002	7722.45	100
0.0002	CR5		1.5449	0.0002	7725	100
0.0002	CR7		1.5453	0.0002	7727	95
0.0002	CR2	Even	1.5443	0.0002	7722	100
0.0002	CR4		1.5447	0.0002	7723.5	100
0.0002	CR6		1.5451	0.0002	7726	95
0.0002	CR8		1.5455	0.0002	7728	100

Table 3. Crosstalk value for the proposed eight-channel demultiplexer (dB).

Channels	λ_1	λ_2	λ_3	λ_4	λ_5	λ_6	λ_7	λ_8
λ_1	—	-54.46	-64	-59	-56	-55.5	-55.3	-51
λ_2	-46.1	—	-53	-58	-57.11	-51.8	-51.2	-51
λ_3	-48	-55	—	-60	-65	-63.3	-52.8	-55.6
λ_4	-44	-55.3	-57	—	-56.9	-55.16	-53.7	-57.8
λ_5	-48.9	-49.8	-60	-49.5	—	-51.4	-48.2	-45.9
λ_6	-55.5	-54.1	-51	-46	-56	—	-46	-47
λ_7	-54	-55	-51	-54	-56	-57	—	55
λ_8	-53	-47	-54	-44	-54	-47	-44	—

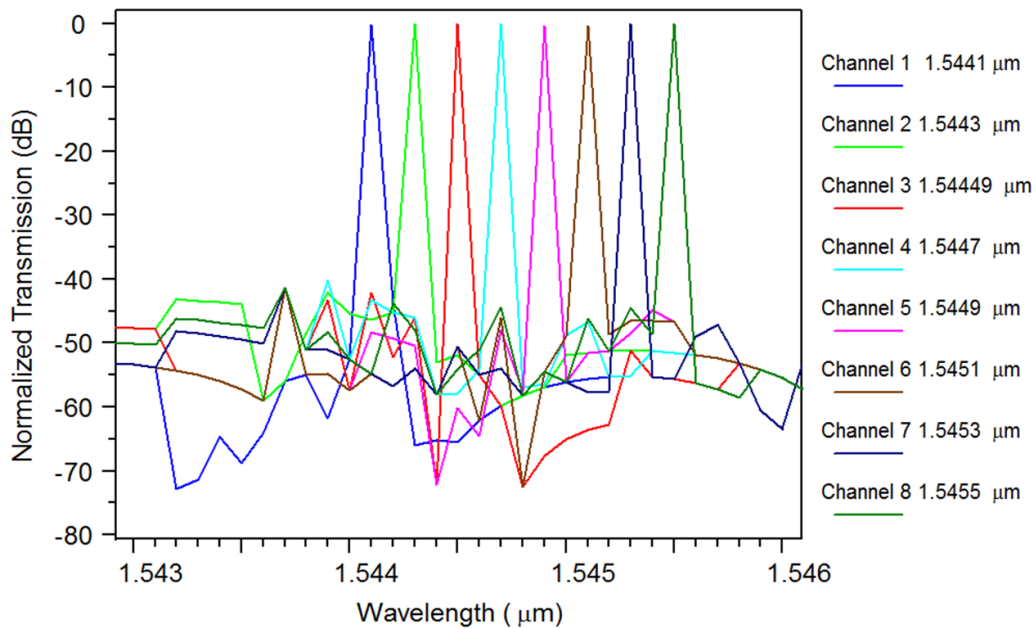


Figure 5. Output spectrum for eight-channel demultiplexer in (dB).

wavelengths are transmitted into the bus waveguide from the fibre. The defects allow the guided mode to transmit inside the waveguide. The light signal is coupled through the ITR and the CR cavity. The CR cavity acts as a resonant region, a specific guided mode transferred to the drop waveguide through the tunnelling effect. According to figure 6, ON resonance is only for a specific wavelength at a particular time. The other CR

cavities act as reflectors, not trapping the photons in the drop waveguide.

The simulation results of the proposed design are compared with the existing paper, shown in table 4. The parameters like lattice type, channel spacing, resonator type, number of channels, transmission efficiency, quality factor, device size, crosstalk, and spectral width are compared. The table

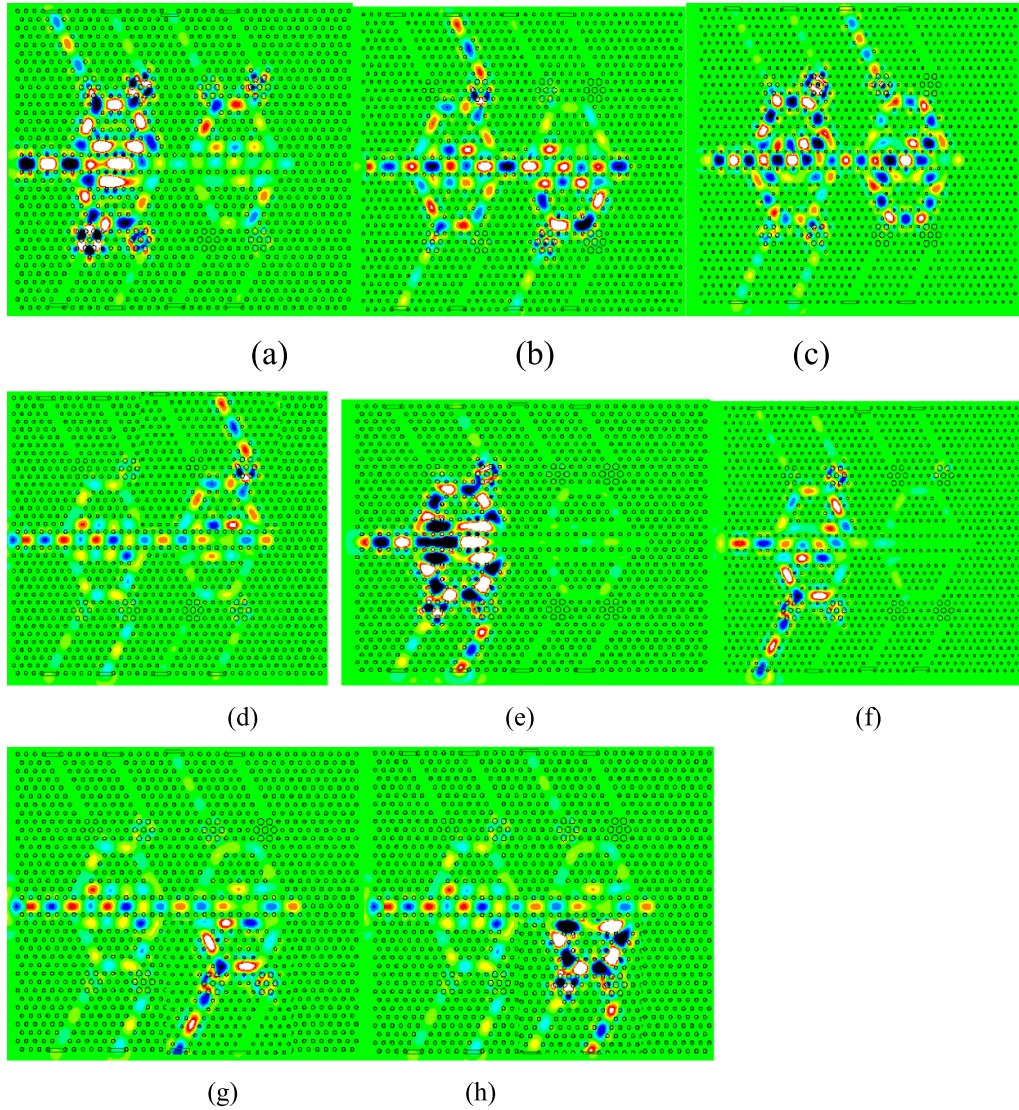


Figure 6. Electric field distribution for (a) channel 1, (b) channel 3, (c) channel 5, (d) channel 7, (e) channel 2, (f) channel 4, (g) channel 6, and (h) channel 8.

clearly states that our proposed design provides uniform channel spacing and spectral width of about $0.0002 \mu\text{m}$, extricating the odd and even channels separately with less crosstalk of -64 dB . Each resonator is designed to drop two different wavelengths, providing a small footprint size of $490 \mu\text{m}^2$. The design provides a high-quality factor of 8000.

5. Salient features of the proposed design and future enhancements

- Each trapezium cavity is designed to drop two resonant wavelengths with a spectral width of 0.2 nm .
- The design is simple and realistic for future photonic integrated circuits.
- The proposed CR cavity limits the different wavelengths by stepping the average rod radius size of 6 nm , the resonant

wavelength selection within channel spacing and spectral width $\leq 0.0001 \mu\text{m}$.

- The design provides minimum Crosstalk of -64 dB and a maximum quality factor of 7728.
- The proposed entire structure design with the same refractive index makes implementation easier.
- A triangular lattice is used for the proposed design; it provides the widest PBG compared to other lattices.
- Scatter rods are not used in the proposed design because it reduces the transmission efficiency and fabrication difficulty during implementation.
- The proposed design primarily employs a trapezium ring resonator without changing the position or periodicity of dielectric rods. Implementing and realizing a trapezium cavity in a triangular lattice is simple.

Table 4. Comparison between proposed eight-channel demultiplexer and previous work.

Reference/ year	Lattice type	Channel spacing (μm) U/NU	Resonator shape	No. of channels	Coupling efficiency (%)		Q factor Max	Device size (μm) ²	Crosstalk (dB) (Min)	Spectral width (μm)	
					Min	Max				Min	Max
[22]/2011	T	3.5 NU	Y	4	63	90	1724	313.28	-33.18	0.9	1.2
[23]/2013	T	3 NU	X	4	45	63	1954	422.4	-22.7	0.8	2.8
[24]/2014	T	1.8 NU	NA	2	92	94	3021	NA	-15	0.5	0.8
[25]/2015	T	0.9 NU	NA	2	100	100	7854	NA	-26.85	0.2	0.3
[26]/2015	T	13 NU	NA	4	73	97	6320	201	-43.9	0.25	0.5
[27]/2017	T	2 NU	Hexagonal	4	93	100	2261.5	424.5	-27	0.7	0.9
[28]/2018	T	2.75 NU	Hexagonal	5	92	100	5272.5	NA	-36.5	0.3	0.55
[29]/2019	T	1.97 NU	Hexagonal	8	91	98.9	1948.7	737	-48.3	0.8	3.2
[30]/2020	T	2 NU	Graphite	4	95	100	3138	289	-27	0.5	0.55
[31]/2021	T	0.8 U	Hexagonal	4	55	60	6000	475	-11.54	NA	NA
This work /2023	T	0.002 U	Trapezium	8	95	100	8582	490	-64	0.18	0.2

T*: triangular lattice U: uniform NU: non-uniform NA: not applicable.

6. Conclusion

In conclusion, we have designed and analysed an eight-channel PC based demultiplexer for DWDM systems. The demultiplexer is designed to drop a uniform narrow spectral width of 0.2 nm for eight channels and works in a conventional window (C window) between the wavelengths of 1.53 μm –1.565 μm . The proposed structure uses the isosceles trapezium as a resonator and a circular cavity as a wavelength-selective filter to drop the desired wavelength to the drop waveguide. The demultiplexer can drop eight consecutive wavelengths with a spectral width of 0.2 nm. Each resonator in the proposed design can drop two wavelengths through the CR cavity and drop the waveguide. The resonator modelled at the top is designed to drop odd channels, and the bottom resonator is designed to drop even channels. The demultiplexer is designed to provide a high transmission efficiency of 100%, a high-quality factor of approximately 8000, and average minimum Crosstalk between channels of -40 dB. The design's footprint is 490 μm^2 and can be easily adapted into PIC.

Data availability statement

The data cannot be made publicly available upon publication because the cost of preparing, depositing and hosting the data would be prohibitive within the terms of this research project. The data that support the findings of this study are available upon reasonable request from the authors.

Acknowledgments

This work was performed on RSoft Bandsolve and FDTD provided by Vellore Institute of Technology, Chennai. The authors are grateful to the institution.

Authors' contributions

The survey and design proposal was verified by V Kavitha, V R Balaji, Shanmuga Sundar Dhanabalan, and T Sridarshini and guided by Gopalkrishna Hegde & S Robinson. Massoudi Radhouene and Jesuwanth Sugesh confirmed the simulation analysis.

Conflict of interest

All the authors hereby confirm that there is no conflict of interest.

Consent to participate

Yes. All equally participated.


Consent for publication

Yes, granted.

ORCID iDs

V Kavitha  <https://orcid.org/0000-0001-7269-0491>

V R Balaji  <https://orcid.org/0000-0002-9239-7724>

Shanmuga Sundar Dhanabalan  <https://orcid.org/0000-0001-5539-3380>

Gopalkrishna Hegde  <https://orcid.org/0000-0003-0197-5873>

R G Jesuwanth Sugesh  <https://orcid.org/0000-0002-2228-8020>

References

- [1] Barry J R, Kahn J M, Lee E A and Messerschmitt D G 1991 High-speed nondirective optical communication for wireless networks *IEEE Netw.* **6** 44–54
- [2] Han J W and Meyyappan M 2014 The device made of nothing *IEEE Spectr.* **7** 30–35
- [3] Fair R B 1990 Challenges to manufacturing submicron, ultra-large scale integrated circuits *Proc. IEEE* **11** 1687–705
- [4] Chau R, Datta S, Doczy M, Doyle B, Jin B, Kavalieros J, Majumdar A, Metz M and Radosavljevic M 2005 Benchmarking nanotechnology for high-performance and low-power logic transistor applications *IEEE Trans. Nanotechnol.* **2** 153–8
- [5] Borella M S, Jue J P, Banerjee D, Ramamurthy B and Mukherjee B 1997 Optical components for WDM lightwave networks *Proc. IEEE* **8** 1274–307
- [6] Norman J C, Jung D, Wan Y and Bowers J E 2018 Perspective: the future of quantum dot photonic integrated circuits *APL Photon.* **3** 030901
- [7] Judy J W 2001 Microelectromechanical systems (MEMS): fabrication, design and applications *Smart Mater. Struct.* **6** 1115
- [8] Mekis A, Chen J C, Kurland I, Fan S, Villeneuve P R and Joannopoulos J D 1996 High transmission through sharp bends in photonic crystal waveguides *Phys. Rev. Lett.* **18** 3787
- [9] Povinelli M L, Johnson S G, Fan S and Joannopoulos J D 2001 Emulation of two-dimensional photonic crystal defect modes in a photonic crystal with a three-dimensional photonic band gap *Phys. Rev. B* **7** 075313
- [10] Woliński T, Ertman S, Lesiak P, Domański A, Czaplą A, Dąbrowski R, Nowinowski-Kruszelnicki E and Wójcik J 2006 Photonic liquid crystal fibers—a new challenge for fiber optics and liquid crystals photonics *Opto-Electron. Rev.* **14** 329–34
- [11] Zhou W *et al* 2014 Progress in 2D photonic crystal Fano resonance photonics *Prog. Quantum Electron.* **1** 1–74
- [12] Lončar M, Scherer A and Qiu Y 2003 Photonic crystal laser sources for chemical detection *Appl. Phys. Lett.* **26** 4648–50
- [13] Liu V, Jiao Y, Miller D A and Fan S 2011 Design methodology for compact photonic-crystal-based wavelength division multiplexers *Opt. Lett.* **4** 591–3
- [14] Balaji V R, Murugan M, Robinson S and Nakkeeran R 2017 Design and optimization of photonic crystal based eight channel dense wavelength division multiplexing demultiplexer using conjugate radiant neural network *Opt. Quantum Electron.* **5** 1–5
- [15] Thirumaran S, Dhanabalan S S and Sannasi I G 2020 Design and analysis of photonic crystal ring resonator based 6x6 wavelength router for photonic integrated circuits *IET Optoelectron.* **15** 40–47

- [16] Salmanpour A, Mohammadnejad S and Bahrami A 2015 Photonic crystal logic gates: an overview *Opt. Quantum Electron.* **7** 2249–75
- [17] Park I, Lee H S, Kim H J, Moon K M, Lee S G, Beom-Hoan O, Park S G and Lee E H 2004 Photonic crystal power-splitter based on directional coupling *Opt. Express* **12** 3599–604
- [18] Zhang J T, Wang L, Luo J, Tikhonov A, Kornienko N and Asher S A 2011 2D array photonic crystal sensing motif *J. Am. Chem. Soc.* **24** 9152–5
- [19] Antil R, Pinki S B and Beniwal S 2012 An overview of DWDM technology & network *Int. J. Sci. Technol. Res.* **11** 43–46
- [20] Lin W, Li H, Chen Y J, Dagenais M and Stone D 1996 Dual-channel-spacing phased-array waveguide grating multi/demultiplexers *IEEE Photonics Technol. Lett.* **11** 1501–3
- [21] Tekeste M Y and Yarrison-Rice J M 2006 High efficiency photonic crystal based wavelength demultiplexer *Opt. Express* **17** 7931–42
- [22] Rostami A, Banaei H A, Nazari F and Bahrami A 2011 An ultra compact photonic crystal wavelength division demultiplexer using resonance cavities in a modified Y-branch structure *Optik* **16** 1481–5
- [23] Alipour-Banaei H, Mehdizadeh F and Serajmohammadi S 2013 A novel 4-channel demultiplexer based on photonic crystal ring resonators *Optik* **23** 5964–7
- [24] Mohammadi B, Soroosh M, Kavsarian A and Mehdizadeh F 2014 A proposed dual channel optical demultiplexer based on photonic crystals *Majlesi J. Telecommun. Devices* **16** 159–62
- [25] Rastegarnia A 2015 Design of optimized structure resonant defects with enhancement ultra-narrow communication channels in two-channel de-multiplexer wavelength photonic crystal to decrease of crosstalk *Majlesi J. Telecommun. Devices* **4** 59–61
- [26] Mehdizadeh F and Soroosh M 2015 A novel proposal for all-optical demultiplexers based on photonic crystal *Optoelectron. Adv. Mater. Commun.* **9** 324–8
- [27] Fallahi V, Seifouri M, Olyae S and Alipour-Banaei H 2017 Four-channel optical demultiplexer based on hexagonal photonic crystal ring resonators *Opt. Rev.* **24** 605–10
- [28] Fallahi V and Seifouri M A 2018 A new design of a 4-channel optical demultiplexer based on photonic crystal ring resonator using a modified Y-branch *Opt. Appl.* **2** 191–200
- [29] Fallahi V, Mohammadi M and Seifouri M 2019 Design of two 8-channel optical demultiplexers using 2D photonic crystal homogeneous ring resonators *Fiber Integr. Opt.* **5** 271–84
- [30] Naghizade S and Mohammadi S 2020 Optical four-channel demultiplexer based on air-bridge structure and graphite-type ring resonators *Photonic Netw. Commun.* **1** 40–48
- [31] Lenin Babu D and Sreenivasulu T 2021 4-Channel DWDM demultiplexer on silicon photonic crystal slab *Sādhanā* **46** 1–4
- [32] Bérenger J P 2007 Perfectly matched layer (PML) for computational electromagnetics *Synth. Lectures Comput. Electromagn.* **1** 1–17
- [33] Yablonovitch E 1994 Photonic crystals *J. Mod. Opt.* **2** 173–94
- [34] Abohassan K M and Ashour H S 2022 Demultiplexers for DWDM applications using one-dimensional planar binary photonic crystals defected with ZnS_xSe_{1-x} ternary alloys *J. Nanophotonics* **16** 016006